Supporting Information for

ORIGINAL ARTICLE

All-stage targeted therapy for the brain metastasis from triple-negative breast cancer

Zimiao Luo[a], Sunyi Wu[a], Jianfen Zhou[a], Weixia Xu[a], Qianzhu Xu[a,b], Linwei Lu[b], Cao Xie[a], Yu Liu[a], Weiyue Lu[a,b,c,*]

[a]*Department of Pharmaceutics, School of Pharmacy, and Key Laboratory of Smart Drug Delivery, Fudan University, Shanghai 201203, & State Key Laboratory of Medical Neurobiology, and Collaborative Innovation Center for Brain Science, Fudan University, Shanghai 200032, China*

[b]*Department of Integrative Medicine, Huashan Hospital, and Institutes of Integrative Medicine of Fudan University, Shanghai 200041, China*

[c]*Minhang Branch, Zhongshan Hospital and Institute of Fudan-Minghang Academic Health System, Minghang Hospital, Fudan University, Shanghai 201199, China*

Received 21 February 2022; received in revised form 28 March 2022; accepted 30 March 2022

[*]Corresponding author.

E-mail address: wylu@shmu.edu.cn (Weiyue Lu).

Supporting Figures S1–S4

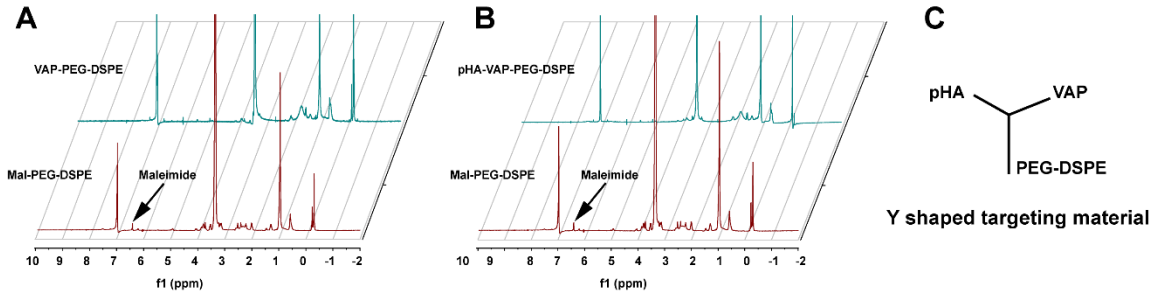

Figure S1 Characterization of the targeting materials. (A) ^{1}H NMR result of VAP-PEG-DSPE; (B) ^{1}H NMR result of pHA-VAP-PEG-DSPE; (C) Schematic diagram of Y-shaped targeting material pHA-VAP-PEG-DSPE.

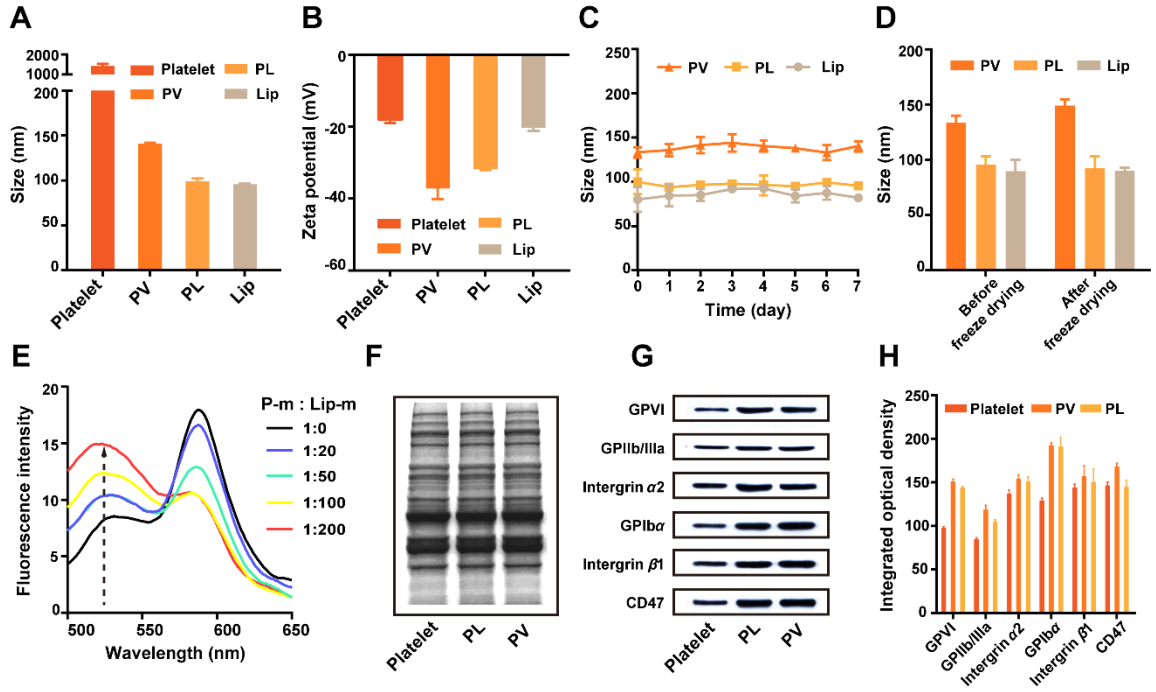

Figure S2 Characterization and examination of membrane fusion and membrane proteins of platelet-hybrid liposomes (PL). Size (A) and zeta potential (B) of PL. Stability of PL in PBS (C) and after freeze drying (D). (E) FRET assay result of fluorescent probes labelled platelet membrane mixing with increasing amounts of lipid. (F) Total protein profiles of PL on SDS-PAGE. Western blotting results (G) and corresponding semiquantitative assay (H) of the markers on platelet membranes in PL. Data are presented as mean ± SD (n = 3).

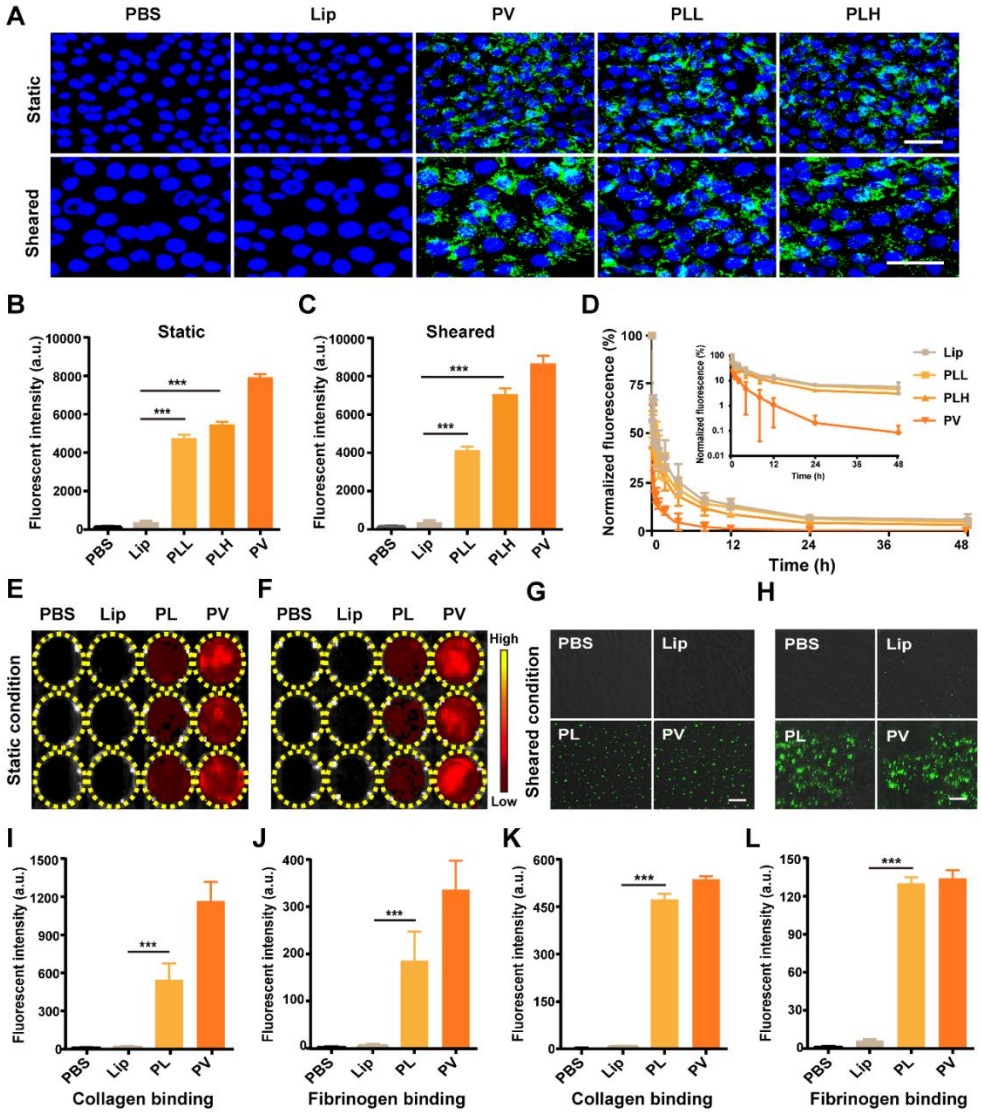

Figure S3 Binding properties and pharmacokinetic behavior of PL. (A) Confocal images of 4T1 cells incubated with PBS or 50 μg/mL of Lip, PV, PLL (low-proportioned platelet membranes) or PLH (high-proportioned platelet membranes) at 4 ℃ for 30 min under a static or shear flow condition (188 s^{-1}). The fluorescent intensity of 4T1 cells in different groups under the static (B) or sheared (C) conditions measured by FACS (n = 3; mean ± SD). (D) The pharmacokinetic profiles of Lip, PhLL, PhLH or PV in mice plasma (8 mg/kg) (n = 5; mean ± SD). The NIR images (E)(F) and quantified results (I)(J) of collagen and fibrinogen binding under a static condition (n = 3; mean ± SD). The NIR images (G)(H) and quantified results (K)(L) of collagen and fibrinogen binding under a sheared condition (500 s^{-1}) (n = 3; mean ± SD). $^{***}P < 0.001$, one-way ANOVA.

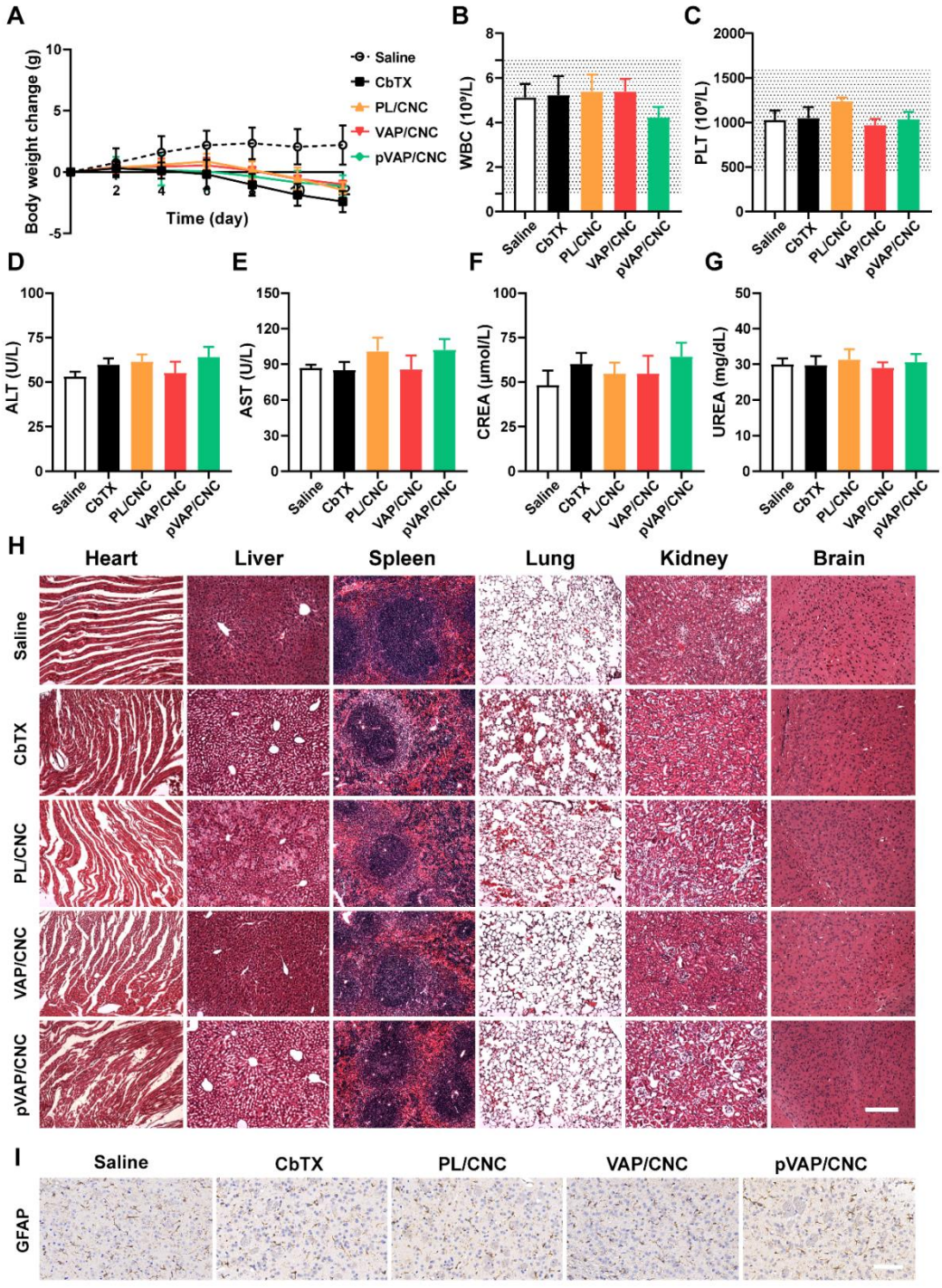

Figure S4 Biosafety evaluation. (A) The body weight changes of mice in different treatment groups (saline, CbTX, PL/CNC, VAP/CNC or pVAP/CNC) during a drug delivery cycle at the total CbTX dose of 18 mg/kg (n = 6; mean ± SD). The hematological analysis (B)(C) and functional assessment of liver (D)(E) and kidney (F)(G) after one time drug injection (n = 4; mean ± SD). (H) The pathological sections of major organs stained by H&E harvested after one time drug injection. (I) GFAP immunohistochemical staining of brain tissue sections from each group. Scale bar = 100 μm.